The POG Technique for Modeling Planetary Gears and Automotive Hybrid Systems

Roberto Zanasi
Information Engineering Department
University of Modena e Reggio Emilia
Via Vignolese 905
41100 Modena, Italy
roberto.zanasi@unimore.it

Federica Grossi
Information Engineering Department
University of Modena e Reggio Emilia
Via Vignolese 905
41100 Modena, Italy
federica.grossi@unimore.it

***Abstract*—In this paper the Power-Oriented Graphs (POG) technique is used for modeling planetary gears and CVT structures within automotive hybrid systems. Some basic properties of the POG technique are given. In particular, the use of congruent state space transformations for reducing the system is analyzed. Some simulation results are finally reported.**

I. Introduction

Nowadays, the planetary gears and the CVT structures are key elements for the design of new hybrid power structures in the automotive area. In this paper the full dynamic models of these systems are obtained using the the POG modeling technique. The obtained dynamic model shows a very compact graphical representation that clearly puts in evidence the power internal structure of the motor. The paper is organized as follows: Sec. II describes the basic properties of the POG modeling technique. Sec. **??** shows how the POG technique can be used for modeling the planetary gears and the CVT structures. Finally, in Sec. **??** some simulation results are reported.

II. Power-Oriented Graphs basic principles

The Power-Oriented Graphs technique, see [1] and [2], is suitable for modeling physical systems. The POG block schemes are normal block diagrams combined with a particular modular structure essentially based on the use of the two blocks shown in Fig. 1.a and Fig. 1.b: the *elaboration block* (e.b.) stores and/or dissipates energy (i.e. springs, masses, dampers, capacities, inductances, resistances, etc.); the *connection block* (c.b.) redistributes the power within the system without storing nor dissipating energy (i.e. any type of gear reduction, transformers, etc.). The e.b. and the c.b. are suitable for representing both scalar and vectorial systems. In the vectorial case, $\mathbf{G}(s)$ and $\mathbf{K}$ are matrices: $\mathbf{G}(s)$ is always a square matrix composed by positive real transfer functions; matrix $\mathbf{K}$ can also be rectangular. The circle present in the e.b. is a summation element and the black spot represents a minus sign that multiplies the entering variable. The main feature of the Power-Oriented Graphs is to keep a direct correspondence between the dashed sections of the graphs and real power sections of the modeled systems: the scalar product $\mathbf{x}^{\mathrm{T}}\mathbf{y}$ of the two *power vectors* $\mathbf{x}$ and $\mathbf{y}$ involved in each dashed line of a power-oriented graph, see Fig. 1, has the physical meaning of *the power flowing through that particular section*. The Bond Graphs technique, see [3], is based on the same idea, but it uses a different and specific graphical representation.

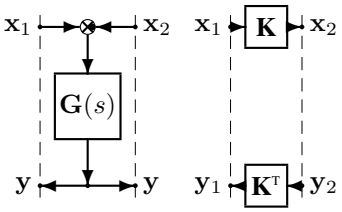

a) *e. b.* b) *c. b.*

	POG Variables	
Domains:	*Across:* v_e	*Through:* v_f
Electrical	Voltage V	Current I
Mec. Tra.	Velocity v	Force F
Mec. Rot.	Ang. Vel. ω	Torque τ
Hydraulic	Pressure P	Flow rate Q

c) *Across and through variables*

Figure 1. POG basic blocks and variables: a) *elaboration block*; b) *connection block*; c) *across and through variables*.

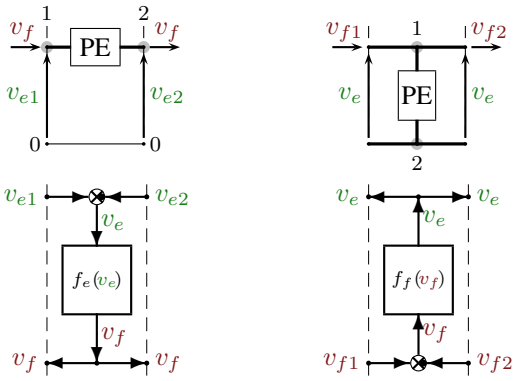

a) Element in series. b) Element in parallel.

Figure 2. POG representations of Physical Elements (PE): a) connected in series (inputs v_{e1}, v_{e2}); b) connected in parallel (inputs v_{f1}, v_{f2}).

The main energetic domains encountered in modeling physical systems are the electrical, the mechanical (translational and rotational) and the hydraulic, see Fig. 1.c. Each energetic domain is characterized by two *power variables*: an *across-variable* v_e defined between two points (i.e. the voltage V), and a *through-variable* v_f defined in each point of the space (i.e. the current I). Each Physical Element (PE) interacts with the external world through the power sections associated

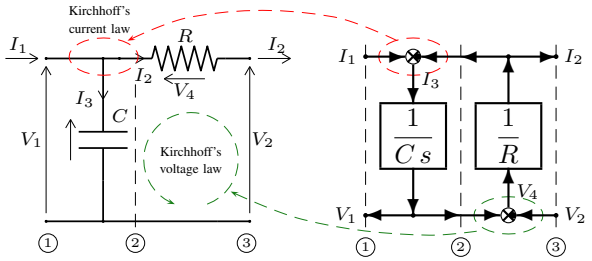

Figure 3. POG modeling of an electrical RC circuit.

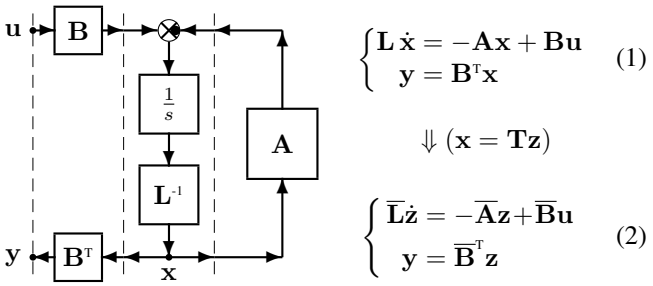

$$\begin{cases} \mathbf{L}\,\dot{\mathbf{x}} = -\mathbf{A}\mathbf{x} + \mathbf{B}\mathbf{u} \\ \mathbf{y} = \mathbf{B}^{\mathrm{T}}\mathbf{x} \end{cases} \tag{1}$$

$$\Downarrow (\mathbf{x} = \mathbf{T}\mathbf{z})$$

$$\begin{cases} \overline{\mathbf{L}}\dot{\mathbf{z}} = -\overline{\mathbf{A}}\mathbf{z} + \overline{\mathbf{B}}\mathbf{u} \\ \mathbf{y} = \overline{\mathbf{B}}^{\mathrm{T}}\mathbf{z} \end{cases} \tag{2}$$

Figure 4. POG block scheme of a generic dynamic system.

to its terminals. A Physical Element is connected *in series* when its terminals share the same through-variable v_f: see the physical element and the corresponding POG scheme in Fig. 2.a. A Physical Element is connected *in parallel* when its terminals share the same across-variable v_e: see the physical element and the POG scheme in Fig. 2.b. An example of POG modeling where a C parallel element is connected with an R series element is shown in Fig. 3. There is a direct corrispondenze between physical power sections and dashed sections in the POG model. Note: the summation elements present in the elaboration blocks are a mathematical description of the current and voltage Kirchhoff's laws applied to the considered electrical system.

Another important property of the POG technique is the direct correspondence between the POG block schemes and the corresponding state space dynamic equations. For example, the POG scheme shown in Fig. 4 can be represented by the state space equations (1) where the *energy matrix* $\mathbf{L}$ is symmetric and positive definite: $\mathbf{L} = \mathbf{L}^{\mathrm{T}} > 0$. When an eigenvalue of matrix $\mathbf{L}$ tends to zero (or to infinity), system (1) degenerates towards a lower dimension dynamic system. In this case, the dynamic model of the "reduced" system, see (2), can be directly obtained from (1) using a simple "congruent" transformation $\mathbf{x} = \mathbf{T}\mathbf{z}$ ($\mathbf{T}$ is constant) where $\overline{\mathbf{L}} = \mathbf{T}^{\mathrm{T}}\mathbf{L}\mathbf{T}$, $\overline{\mathbf{A}} = \mathbf{T}^{\mathrm{T}}\mathbf{A}\mathbf{T}$ and $\overline{\mathbf{B}} = \mathbf{T}^{\mathrm{T}}\mathbf{B}$.

A. POG modeling of a planetary gear

Let us consider the planetary gear shown in Fig. 5 together with the main parameters of the system. The extended POG dynamic model of the considered planetary gear is shown in Fig. 6: the carrier, the planets and the ring interact each other through two elastic elements. The corresponding state space

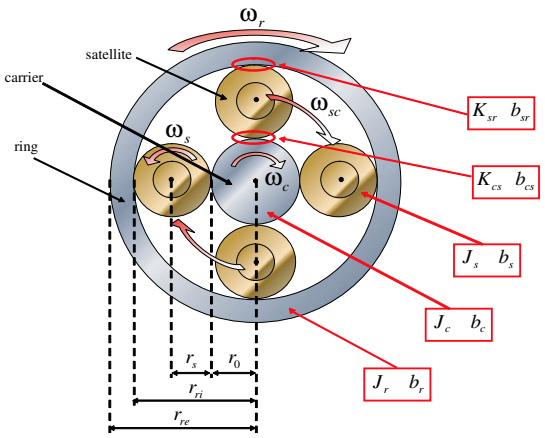

Figure 5. Planetary gear and related parameters.

dynamic equations are shown in Fig. 7:

$$\overline{\mathbf{L}}\,\dot{\overline{\mathbf{x}}} = -\overline{\mathbf{A}}\,\overline{\mathbf{x}} + \overline{\mathbf{B}}\,\mathbf{u}, \qquad \mathbf{y} = \overline{\mathbf{B}}^{\mathrm{T}}\overline{\mathbf{x}} \tag{3}$$

The POG linear systems described in the form (3) satisfy the following properties: 1) the energy E_s stored in the system and the dissipating power P_d can be expressed as quadratic functions of matrices $\overline{\mathbf{L}}$ and $\overline{\mathbf{A}}_s$ as follows:

$$E_s = \frac{1}{2}\,\overline{\mathbf{x}}^{\mathrm{T}}\,\overline{\mathbf{L}}\,\overline{\mathbf{x}}, \qquad P_d = \overline{\mathbf{x}}^{\mathrm{T}}\,\overline{\mathbf{A}}_s\,\overline{\mathbf{x}}$$

where $\overline{\mathbf{A}}_s = (\overline{\mathbf{A}} + \overline{\mathbf{A}}^{\mathrm{T}})/2$ is the symmetric part of the *power matrix* $\overline{\mathbf{A}}$. The skew-symmetric part $\overline{\mathbf{A}}_w = (\overline{\mathbf{A}} - \overline{\mathbf{A}}^{\mathrm{T}})/2$ of matrix $\overline{\mathbf{A}}$ represents power redistribution within the system. A POG scheme always satisfies the following two rules: 1) *along all the loops of the scheme must be present an "odd" number of signs "−"* (the black spots in the summation blocks); 2) *the direction of the power flowing through a section is positive if an "even" number of signs "−" is present along all the paths which link the input to the output*.

For certain applications the POG model of Fig. 6 can be too much detailed. In these cases it can be of interest to find the reduced model when the stiffness coefficients K_{sr} and K_{sc} tend to infinity. Applying to system (3) the following congruent transformation:

$$\overline{\mathbf{x}} = \mathbf{T}_1\,\mathbf{x}, \qquad \text{where} \qquad \mathbf{T}_1 = \begin{bmatrix} 1&0&0&0&0&0 \\ 0&0&0&0&0&1 \\ 0&0&1&0&0&0 \\ 0&1&0&0&0&0 \\ 0&0&0&0&1&0 \\ 0&0&0&1&0&0 \end{bmatrix}.$$

one easily obtains the following transformed system:

$$\underbrace{\begin{bmatrix} \mathbf{J}_1 & 0 & 0 \\ 0 & \mathbf{J}_2 & 0 \\ 0 & 0 & 0 \end{bmatrix}}_{\mathbf{L}} \underbrace{\begin{bmatrix} \dot{\mathbf{x}}_1 \\ \dot{\mathbf{x}}_2 \\ \dot{\mathbf{x}}_3 \end{bmatrix}}_{\dot{\mathbf{x}}} = -\underbrace{\begin{bmatrix} \mathbf{A}_{11} & \mathbf{A}_{12} & \mathbf{A}_{13} \\ \mathbf{A}_{21} & \mathbf{A}_{22} & \mathbf{A}_{23} \\ \mathbf{A}_{31} & \mathbf{A}_{32} & 0 \end{bmatrix}}_{\mathbf{A}} \underbrace{\begin{bmatrix} \mathbf{x}_1 \\ \mathbf{x}_2 \\ \mathbf{x}_3 \end{bmatrix}}_{\mathbf{x}} + \underbrace{\begin{bmatrix} \mathbf{B}_1 \\ \mathbf{B}_2 \\ 0 \end{bmatrix}}_{\mathbf{B}} \mathbf{u} \tag{4}$$

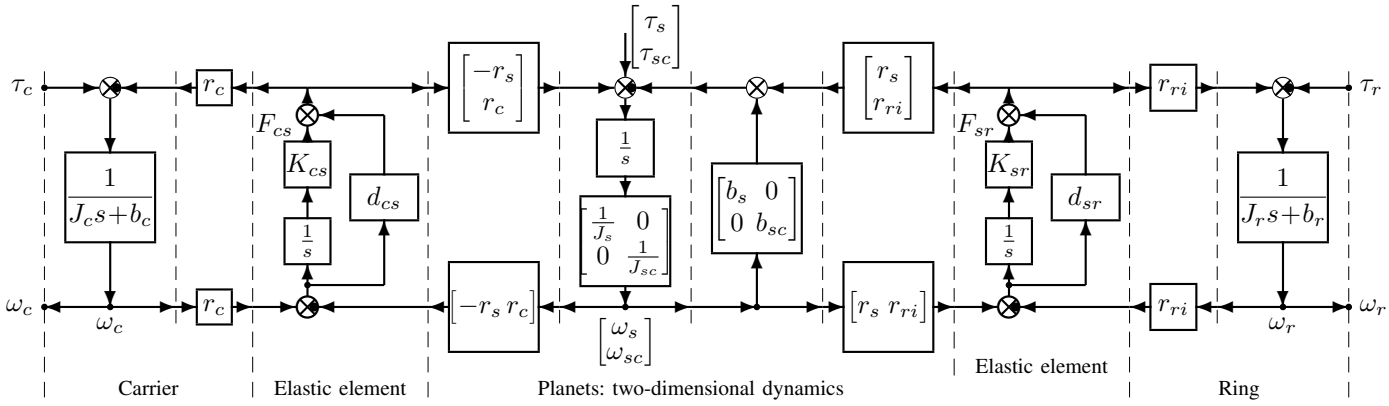

Figure 6. The POG model of the considered planetary gear: the carrier, the planets and the ring interact through elastic elements.

$$\underbrace{\begin{bmatrix} J_c & 0 & 0 & 0 & 0 & 0 \\ 0 & \frac{1}{K_{cs}} & 0 & 0 & 0 & 0 \\ 0 & 0 & J_s & 0 & 0 & 0 \\ 0 & 0 & 0 & J_{sc} & 0 & 0 \\ 0 & 0 & 0 & 0 & \frac{1}{K_{sr}} & 0 \\ 0 & 0 & 0 & 0 & 0 & J_r \end{bmatrix}}_{\overline{\mathbf{L}}} \underbrace{\begin{bmatrix} \dot{\omega}_c \\ \dot{F}_{cs} \\ \dot{\omega}_s \\ \dot{\omega}_{sc} \\ \dot{F}_{sr} \\ \dot{\omega}_r \end{bmatrix}}_{\dot{\overline{\mathbf{x}}}} = -\underbrace{\begin{bmatrix} b_c+r_c^2 d_{cs} & r_c & r_c d_{cs} r_s & -r_c^2 d_{cs} & 0 & 0 \\ -r_c & 0 & -r_s & r_c & 0 & 0 \\ r_c d_{cs} r_s & r_s & b_s+d_{cs} r_s^2+d_{sr} r_s^2 & -r_c d_{cs} r_s+d_{sr} r_s r_{ri} & r_s & -d_{sr} r_s r_{ri} \\ -r_c^2 d_{cs} & -r_c & r_c d_{cs} r_s+d_{sr} r_s r_{ri} & b_{sc}+r_c^2 d_{cs}+d_{sr} r_{ri}^2 & r_{ri} & -d_{sr} r_{ri}^2 \\ 0 & 0 & -r_s & r_{ri} & 0 & r_{ri} \\ 0 & 0 & -d_{sr} r_s r_{ri} & -d_{sr} r_{ri}^2 & -r_{ri} & b_r+d_{sr} r_{ri}^2 \end{bmatrix}}_{\overline{\mathbf{A}}} \underbrace{\begin{bmatrix} \omega_c \\ F_{cs} \\ \omega_s \\ \omega_{sc} \\ F_{sr} \\ \omega_r \end{bmatrix}}_{\overline{\mathbf{x}}} + \underbrace{\begin{bmatrix} 1 & 0 & 0 \\ 0 & 0 & 0 \\ 0 & 0 & 0 \\ 0 & 1 & 0 \\ 0 & 0 & 0 \\ 0 & 0 & 1 \end{bmatrix}}_{\overline{\mathbf{B}}} \underbrace{\begin{bmatrix} \tau_c \\ \tau_{sc} \\ \tau_r \end{bmatrix}}_{\mathbf{u}}$$

Figure 7. The POG state space dynamic model of the considered planetary gear: only the inputs τ_c, τ_{sc} and τ_r have been considered.

where $\mathbf{x} = \mathbf{T}_1^{\mathrm{T}}\,\overline{\mathbf{x}}$, $\mathbf{L} = \mathbf{T}_1^{\mathrm{T}}\overline{\mathbf{L}}\,\mathbf{T}_1$, $\mathbf{B} = \mathbf{T}_1^{\mathrm{T}}\,\overline{\mathbf{B}}$ and $\mathbf{A} = \mathbf{T}_1^{\mathrm{T}}\overline{\mathbf{A}}\,\mathbf{T}_1$ and where:

$$\mathbf{x}_1 = \begin{bmatrix} \omega_c \\ \omega_{sc} \end{bmatrix},\ \mathbf{x}_2 = \begin{bmatrix} \omega_s \\ \omega_r \end{bmatrix},\ \mathbf{x}_3 = \begin{bmatrix} F_{sr} \\ F_{cs} \end{bmatrix},\ \mathbf{J}_1 = \begin{bmatrix} J_c & 0 \\ 0 & J_{sc} \end{bmatrix},\ \mathbf{J}_2 = \begin{bmatrix} J_s & 0 \\ 0 & J_r \end{bmatrix},$$

$$\mathbf{B}_1 = \begin{bmatrix} 1 & 0 & 0 \\ 0 & 1 & 0 \end{bmatrix},\ \mathbf{B}_2 = \begin{bmatrix} 0 & 0 & 0 \\ 0 & 0 & 1 \end{bmatrix},\ \mathbf{A}_{11} = \begin{bmatrix} b_c+r_c^2 d_{cs} & -r_c^2 d_{cs} \\ -r_c^2 d_{cs} & b_{sc}+r_c^2 d_{cs}+d_{sr} r_{ri}^2 \end{bmatrix},$$

$$\mathbf{A}_{12} = \begin{bmatrix} r_c d_{cs} r_s & 0 \\ -r_c d_{cs} r_s+d_{sr} r_s r_{ri} & -d_{sr} r_{ri}^2 \end{bmatrix},\ \mathbf{A}_{13} = \begin{bmatrix} 0 & r_c \\ r_{ri} & -r_c \end{bmatrix},\ \mathbf{A}_{31} = \begin{bmatrix} 0 & -r_{ri} \\ -r_c & r_c \end{bmatrix},$$

$$\mathbf{A}_{21} = \begin{bmatrix} r_c d_{cs} r_s & -r_c d_{cs} r_s+d_{sr} r_s r_{ri} \\ 0 & -d_{sr} r_{ri}^2 \end{bmatrix},\qquad \mathbf{A}_{23} = \begin{bmatrix} r_s & r_s \\ -r_{ri} & 0 \end{bmatrix},$$

$$\mathbf{A}_{22} = \begin{bmatrix} b_s+d_{cs} r_s^2+d_{sr} r_s^2 & -d_{sr} r_s r_{ri} \\ -d_{sr} r_s r_{ri} & b_r+d_{sr} r_{ri}^2 \end{bmatrix},\qquad \mathbf{A}_{32} = \begin{bmatrix} -r_s & r_{ri} \\ -r_s & 0 \end{bmatrix},$$

The last equation of system (4) shows an algebraic relation between the state variables: $\mathbf{A}_{31}\,\mathbf{x}_1 + \mathbf{A}_{32}\,\mathbf{x}_2 = 0$. Since matrix $\mathbf{A}_{32}$ is invertible, vector $\mathbf{x}_2$ can be expressed as: $\mathbf{x}_2 = -\mathbf{A}_{32}^{-1}\,\mathbf{A}_{31}\,\mathbf{x}_1$. Applying to system (4) the following "rectangular" transformation:

$$\mathbf{x} = \mathbf{T}_2\,\mathbf{x}_1 \quad \text{where} \quad \mathbf{T}_2 = \begin{bmatrix} \mathbf{I}_2 \\ -\mathbf{A}_{32}^{-1}\,\mathbf{A}_{31} \\ 0 \end{bmatrix} = \begin{bmatrix} 1 & 0 \\ 0 & 0 \\ -\frac{r_c}{r_s} & \frac{r_c}{r_s} \\ -\frac{r_c}{r_{ri}} & 1+\frac{r_c}{r_{ri}} \\ 0 & 0 \\ 0 & 0 \end{bmatrix}$$

one obtains the following second order transformed and reduced system:

$$\mathbf{L}_r\,\dot{\mathbf{x}}_1 = -\mathbf{A}_r\,\mathbf{x}_1 + \mathbf{B}_r\,\mathbf{u}, \qquad \mathbf{y} = \mathbf{B}_r^{\mathrm{T}}\mathbf{x}_1 \tag{5}$$

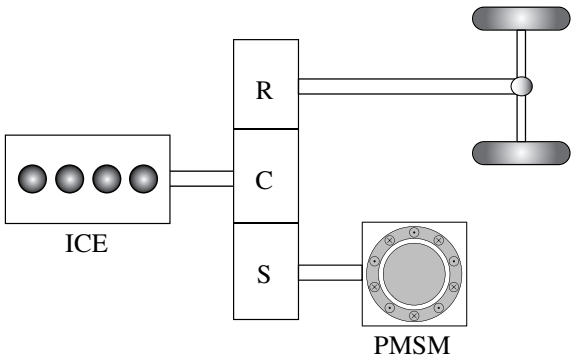

Figure 8. Scheme of the considered power structure of the vehicle

where

$$\mathbf{L}_r = \begin{bmatrix} J_c+\frac{r_c^2}{r_s^2} J_s+\frac{r_c^2}{r_{ri}^2} J_r & -\frac{r_c^2}{r_s^2} J_s-\frac{r_c}{r_{ri}}\left(1+\frac{r_c}{r_{ri}}\right) J_r \\ -\frac{r_c^2}{r_s^2} J_s-\frac{r_c}{r_{ri}}\left(1+\frac{r_c}{r_{ri}}\right) J_r & J_{sc}+\frac{r_c^2}{r_s^2} J_s+\left(1+\frac{r_c}{r_{ri}}\right)^2 J_r \end{bmatrix}$$

$$\mathbf{A}_r = \begin{bmatrix} b_c+\frac{r_c^2}{r_s^2} b_s+\frac{r_c^2}{r_{ri}^2} b_r & -\left(1+\frac{r_c}{r_{ri}}\right)\left(1+\frac{r_c}{r_{ri}} b_r\right)-\frac{r_c^2}{r_s^2} b_s \\ \left(1+\frac{r_c}{r_{ri}}\right)\left(1-\frac{r_c}{r_{ri}} b_r\right)-\frac{r_c^2}{r_s^2} b_s & b_{sc}+\frac{r_c^2}{r_s^2} b_s+\left(1+\frac{r_c}{r_{ri}}\right)^2 b_r \end{bmatrix}$$

$$\mathbf{B}_r = \begin{bmatrix} 1 & 0 & -\frac{r_c}{r_{ri}} \\ 0 & 1 & 1+\frac{r_c}{r_{ri}} \end{bmatrix}, \quad \mathbf{x}_1 = \begin{bmatrix} \omega_c \\ \omega_{sc} \end{bmatrix}, \quad \mathbf{y} = \begin{bmatrix} \tau_c \\ \tau_{sc} \\ \tau_r \end{bmatrix}$$

III. POG MODELING OF AN AUTOMOTIVE HYBRID SYSTEM

The planetary gear is the key element for modeling the hybrid powertrain structure shown in Fig. 8. The considered vehicle structure includes an internal combustion engine (ICE)

and a multi-phase permanent magnet synchronous machine (PMSM). The planetary gear is introduced as the element connecting the two motors and the driving wheels. The ICE is connected to the Carrier (C), the PMSM is connected to the Planet Carrier (S) and the driving axle is connected to the Ring (R).

IV. Simulation

The system shown in Fig. 8 has been implemented in Matlab/Simulink as it is shown in Fig. 9. All subsystems have been modeled with POG and in particular the vehicle subsystem in the right part of the scheme is a bicycle model of a car that includes the tire-road elastic interaction, see [5].

V. Conclusions

In this paper the Power-Oriented Graphs (POG) technique has benn used for modeling ...

References

[1] R. Zanasi, "Power Oriented Modelling of Dynamical System for Simulation", IMACS Symp. on Modelling and Control of Technological System, Lille, France, May 1991.

[2] Zanasi R., "Dynamics of a n-links Manipulator by Using Power-Oriented Graph", *SYROCO '94*, Capri, Italy, 1994.

[3] D. C. Karnopp, D.L. Margolis, R. C. Rosemberg, *System dynamics - Modeling and Simulation of Mechatronic Systems*, Wiley Interscience, ISBN 0-471-33301-8, 3rd ed. 2000.

[4] R. Zanasi, F. Grossi "Optimal Rotor Flux Shape for Multi-phase Permanent Magnet Synchronous Motors", International Power Electronics and Motion Control Conference, September 1-3 2008, Poznan, Poland.

[5] F. Grossi, W. Lhomme, R. Zanasi, A. Bouscayrol, "Modelling and control of a vehicle with tire-road interaction using POG and EMR formalisms", accepted to Electromotion 2009, EPE chapter Electric Drives, 1-3 July 2009, Lille, France

$$\underbrace{\begin{bmatrix} L_1 & L_{12} \\ L_{12} & L_2 \end{bmatrix}}_{\mathbf{L}_r} \underbrace{\begin{bmatrix} \dot{\omega}_c \\ \dot{\omega}_{sc} \end{bmatrix}}_{\dot{\mathbf{x}}_1} = - \underbrace{\begin{bmatrix} a_{11} & a_{12} \\ a_{21} & a_{22} \end{bmatrix}}_{\mathbf{A}_r} \underbrace{\begin{bmatrix} \omega_c \\ \omega_{sc} \end{bmatrix}}_{\mathbf{x}_1} + \underbrace{\begin{bmatrix} 1 & 0 & b_1 \\ 1 & 0 & b_2 \end{bmatrix}}_{\mathbf{B}_r} \mathbf{u} \quad (6)$$

where

$$\begin{aligned}
L_1 &= J_c + \tfrac{r_c^2}{r_s^2} J_s + \tfrac{r_c^2}{r_{ri}^2} J_r \\
L_{12} &= -\tfrac{r_c^2}{r_s^2} J_s - \tfrac{r_c}{r_{ri}} \left(1 + \tfrac{r_c}{r_{ri}}\right) J_r \\
L_2 &= J_{sc} + \tfrac{r_c^2}{r_s^2} J_s + \left(1 + \tfrac{r_c}{r_{ri}}\right)^2 J_r \\
a_{11} &= b_c + \tfrac{r_c^2}{r_s^2} b_s + \tfrac{r_c^2}{r_{ri}^2} b_r \\
a_{12} &= -1 - \tfrac{r_c}{r_{ri}} - \tfrac{r_c^2}{r_s^2} b_s - \tfrac{r_c}{r_{ri}} \left(1 + \tfrac{r_c}{r_{ri}}\right) b_r \\
a_{21} &= 1 + \tfrac{r_c}{r_{ri}} - \tfrac{r_c^2}{r_s^2} b_s - \tfrac{r_c}{r_{ri}} \left(1 + \tfrac{r_c}{r_{ri}}\right) b_r \\
a_{22} &= b_{sc} + \tfrac{r_c^2}{r_s^2} b_s + \left(1 + \tfrac{r_c}{r_{ri}}\right)^2 b_r \\
b_1 &= \tfrac{-r_c}{r_{ri}} \\
b_2 &= 1 + \tfrac{r_c}{r_{ri}}
\end{aligned}$$

$$\begin{aligned}
L_1 &= J_c + \tfrac{r_c^2}{r_s^2} J_s + \tfrac{r_c^2}{r_{ri}^2} J_r \\
L_{12} &= -\tfrac{r_c^2}{r_s^2} J_s - \tfrac{r_c}{r_{ri}} \left(1 + \tfrac{r_c}{r_{ri}}\right) J_r \\
L_2 &= J_{sc} + \tfrac{r_c^2}{r_s^2} J_s + \left(1 + \tfrac{r_c}{r_{ri}}\right)^2 J_r \\
a_{11} &= b_c + \tfrac{r_c^2}{r_s^2} b_s + \tfrac{r_c^2}{r_{ri}^2} b_r \\
a_{12} &= -\left(1 + \tfrac{r_c}{r_{ri}}\right)\left(1 + \tfrac{r_c}{r_{ri}} b_r\right) - \tfrac{r_c^2}{r_s^2} b_s \\
a_{21} &= \left(1 + \tfrac{r_c}{r_{ri}}\right)\left(1 - \tfrac{r_c}{r_{ri}} b_r\right) - \tfrac{r_c^2}{r_s^2} b_s \\
a_{22} &= b_{sc} + \tfrac{r_c^2}{r_s^2} b_s + \left(1 + \tfrac{r_c}{r_{ri}}\right)^2 b_r \\
b_1 &= -\tfrac{r_c}{r_{ri}} \\
b_2 &= 1 + \tfrac{r_c}{r_{ri}}
\end{aligned}$$

$$\begin{aligned}
L_1 &= J_c + \rho^2 J_s + \delta^2 J_r \\
L_{12} &= -\rho^2 J_s - \delta\,(1+\delta)\, J_r \\
L_2 &= J_{sc} + \rho^2 J_s + (1+\delta)^2 J_r \\
a_{11} &= b_c + \rho^2 b_s + \delta^2 b_r \\
a_{12} &= -1 - \delta - \rho^2 b_s - \delta\,(1+\delta)\, b_r \\
a_{21} &= 1 + \delta - \rho^2 b_s - \delta\,(1+\delta)\, b_r \\
a_{22} &= b_{sc} + \rho^2 b_s + (1+\delta)^2 b_r \\
b_1 &= -\delta \\
b_2 &= 1 + \delta
\end{aligned}$$

where

$$\rho = \frac{r_c}{r_s}, \qquad \delta = \frac{r_c}{r_{ri}}, \qquad \gamma = 1 + \delta$$

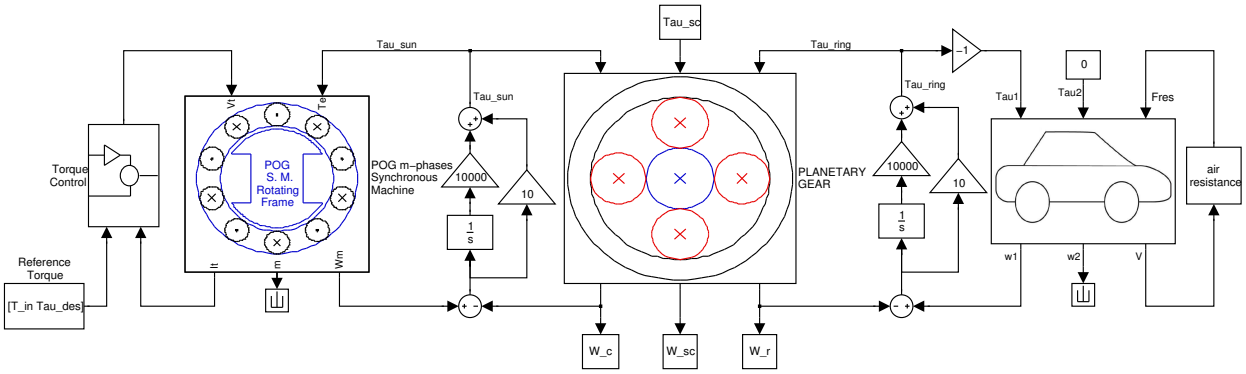

Figure 9. Scheme of the considered vehicle

$$
\begin{aligned}
L_1 &= J_c + \rho_s^2 J_s + \rho_r^2 J_r \\
L_{12} &= -\rho_s^2 J_s - \rho_r \gamma_r J_r \\
L_2 &= J_{sc} + \rho_s^2 J_s + \gamma_r^2 J_r \\
a_{11} &= b_c + \rho_s^2 b_s + \rho_r^2 b_r \\
a_{12} &= -\gamma_r - \rho_s^2 b_s - \rho_r \gamma_r b_r \\
a_{21} &= \gamma_r - \rho_s^2 b_s - \rho_r \gamma_r b_r \\
a_{22} &= b_{sc} + \rho_s^2 b_s + \gamma_r^2 b_r \\
b_1 &= -\rho_r \\
b_2 &= \gamma_r
\end{aligned}
$$

where

$$\rho_s = \frac{r_c}{r_s}, \qquad \rho_r = \frac{r_c}{r_{ri}}, \qquad \gamma_r = 1 + \rho_r$$

dove

$$\mathbf{L}_r = \begin{bmatrix} J_c + \rho_s^2 J_s + \rho_r^2 J_r & -\rho_s^2 J_s - \rho_r \gamma_r J_r \\ -\rho_s^2 J_s - \rho_r \gamma_r J_r & J_{sc} + \rho_s^2 J_s + \gamma_r^2 J_r \end{bmatrix}$$

$$\mathbf{A}_r = \begin{bmatrix} b_c + \rho_s^2 b_s + \rho_r^2 b_r & -\gamma_r - \rho_s^2 b_s - \rho_r \gamma_r b_r \\ \gamma_r - \rho_s^2 b_s - \rho_r \gamma_r b_r & b_{sc} + \rho_s^2 b_s + \gamma_r^2 b_r \end{bmatrix}$$

$$\mathbf{B}_r = \begin{bmatrix} 1 & 0 & -\rho_r \\ 0 & 1 & \gamma_r \end{bmatrix}, \quad \rho_s = \frac{r_c}{r_s}, \quad \rho_r = \frac{r_c}{r_{ri}}, \quad \gamma_r = 1 + \rho_r.$$